Droop-Free Distributed Frequency Control of Hybrid PV-BES Microgrid with SOC Balancing and Active Power Sharing

¹Sheik M. Mohiuddin, ²Amirthagunaraj Yogarathnam, ²Meng Yue, and ¹Junjian Qi ¹Department of Electrical and Computer Engineering, Stevens Institute of Technology, Hoboken, NJ, USA ²Sustainable Energy Technologies Department, Brookhaven National Laboratory, Upton, NY, USA Emails: smohiudd@stevens.edu, ayogarath@bnl.gov, yuemeng@bnl.gov, jqi8@stevens.edu

Abstract—In this paper, we propose a droop-free distributed frequency control for the hybrid photovoltaic and battery energy storage (PV-BES) based microgrid. A distributed state of charge (SOC) balancing regulator achieves balanced SOC among the distributed generators (DGs) with BES utilizing a distributed average SOC estimator and the power sharing regulator ensures proportional power sharing among the PV-BES based DGs. These regulators generate two frequency correction terms which are then added to the microgrid rated frequency to generate references for the lower level controllers. The performance of the proposed distributed control is validated through real-time simulations in OPAL-RT, which demonstrates the effectiveness of the proposed control in achieving frequency regulation, SOC balancing, and active power sharing in the hybrid PV-BES units under both islanded and grid-connected operation modes.

I. Introduction

The penetration of distributed generators (DGs) based on renewable energy resources (RESs) is increasing at a rapid pace due to the concerns for climate change and energy sustainability. However, the power output from RESs has intrinsic intermittency and fluctuation due to dependence on environmental conditions, which unavoidably poses significant challenges on power quality and reliability [1]. The hybrid DG units comprising RESs and battery energy storage (BES) units (e.g., PV-BES) with appropriate control algorithms are one of the preferred solutions to address these issues. The hybrid PV-BES units can also be used for peak shaving and peak shifting, grid efficiency improvement, and congestion relief [2].

Traditionally, in a PV-BES configuration, depending on the state of charge (SOC) level of the BES and/or the system loading conditions, the PV plant can be operated either in maximum power point tracking (MPPT) mode or powersharing mode [3]. If the hybrid PV-BES is connected to the AC microgrid, defining control strategies based on SOC and the loading conditions may increase the complexity of the control algorithm. Moreover, in order to prevent deterioration of the BES due to frequent charging/discharging and over stressing, the SOCs of the BESs need to be balanced [2].

This work was supported by the Advanced Grid Modeling Program of the Office of Electricity, the Department of Energy and the Laboratory Directed Research and Development Program, Brookhaven National Laboratory. J. Qi's work was supported by the National Science Foundation under Grant No. ECCS-2103426.

For coordination among the hybrid sources and achieving SOC balancing, centralized [4], decentralized [5], and distributed [2] approaches have been proposed. The centralized controls are susceptible to single point failure [6] and incur computational burden and increased implementation costs [7]. The decentralized control in [5] utilizes the power-frequency droop for power management. However, the droop control provides poor dynamic performance, susceptible to measurement noises, and may lead to unsuitable voltage and/or power regulations under nonlinear loads [6]. By contrast, distributed control utilizes a sparse communication structure and has reduced computational burden and high reliability [7].

The authors in [2] propose a distributed multi-agent based control for multiple energy storage systems in an AC microgrid. The SOC balancing approach in [2] uses a distributed SOC estimator based on which the output frequencies of the DGs are updated using a droop control. However, this approach does not consider PV or BES on the DC side which simplifies the control problem as for hybrid PV-BES configuration the charging and discharging cycles of the battery depends on the PV output and the system loading conditions. In [8], a distributed secondary control is proposed for SOC balancing, power sharing, and voltage regulation of a hybrid PV-BES based AC microgrid. However, the primary control relies on V-I droop strategy and thus has the aforementioned limitations.

In this paper, we propose a droop-free distributed frequency control with SOC balancing and active power sharing for a hybrid PV-BES based microgrid. The main contributions of the paper are summarized as follows.

- A SOC balancing regulator based on a distributed average SOC estimator for the DGs with BES is designed to ensure SOC balancing among the BES units.
- An active power sharing regulator is designed to achieve proportional power sharing among hybrid PV-BES based DGs, considering the power rating of both PV and BES.
- 3) Steady-state analysis of the proposed control is performed to show that all design objectives can be achieved. The performance of the proposed control is validated through real-time simulations in OPAL-RT.

The remainder of this paper is organized as follows. Section II introduces the cyber-physical model of the microgrid. The

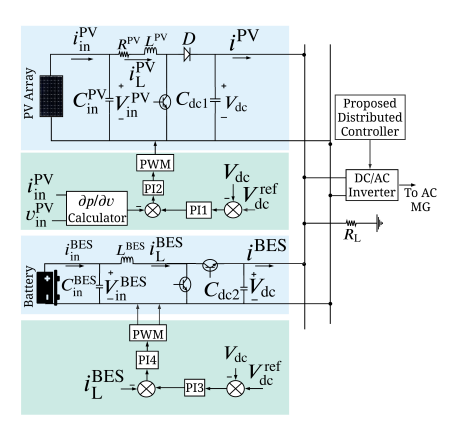


Fig. 1. The schematic of hybrid PV-BES plant with its DC-side converters' controls.

proposed distributed frequency control is presented in Section III. Steady-state analysis of the proposed control is discussed in Section IV. The control performance is then demonstrated through real-time simulations in Section V and finally conclusions are drawn in Section VI.

II. CYBER-PHYSICAL NETWORK OF THE MICROGRID

A. Physical Network Modeling

In this study, the physical network considers a detailed 3-phase modeling of a microgrid, which consists of N hybrid PV-BES plants with its controls, loads and three-phase lines. The detailed description of a hybrid PV-BES plant considered in this study is shown in Fig. 1. The PV and BES are connected to the DC bus via a boost and a buck-boost converters, respectively. Then a DC-AC inverter connects them to the AC network. For generality we assume that a hybrid PV-BES plant may or may not include a BES, indicated by k_i where $k_i=1$ if the hybrid DG i has BES and $k_i=0$ otherwise. Assume the number of hybrid plants with BES is \tilde{N} and the set of hybrid plants with BES is denoted by \mathcal{N}^{BES} .

In this paper, a distributed control for the DC-AC inverter is proposed, which will be discussed in Section III. The control signal from the proposed control is sent to the PWM of the DC-AC inverter. The controls of the DC-DC boost converter and the DC-DC buck-boost converter are discussed below.

- 1) DC-DC boost converter with unified MPPT and voltage regulation: Traditionally in hybrid PV-BES system the DC-DC boost converters for PVs are operated in the following three different modes [3], [5].
 - Mode 1: If the total load is more than the available PV generation, the PV operates in MPPT mode and the BES injects the additional power required by power balance.
 - Mode 2: If the total load is less than the PV generation and the BES has the capacity to absorb additional power, then the PV still operates in MPPT mode.
 - Mode 3: If the total PV generation is more than the total load and the BES has been charged to its maximum capacity, then the PV operates in load sharing mode.

These controls depend on the load demand and PV power output, and the complexity in these modes of operations may

increase with the elevated SOC level of the BES. Furthermore, the BESs may need to be disconnected from the hybrid system or may fail to regulate the DC bus voltage after exceeding their charging/discharging limits [9].

Therefore, in this paper, using the voltage regulation and the $\partial p/\partial v$ (i.e., the partial derivative of the power with respect to the voltage magnitude), a unified control for the DC-DC boost converter is implemented as shown in Fig. 1. The voltage control-loop regulates the DC-side voltage and the $\partial p/\partial v$ control-loop enables MPPT for the PV [9]. It should be noted that at the point of MPPT the $\partial p/\partial v$ becomes zero. Therefore, the unified control ensures that the PV operates for voltage regulation and MPPT in Modes 1 and 2. On the other hand, it ensures voltage regulation in Mode 3.

2) DC-DC buck-boost converter: The control of the DC-DC buck-boost converter is shown in Fig. 1. In this study, the control for the battery converters is implemented using the outer voltage and inner current control loops to mitigate the impact of the nonlinear relation between battery voltage and the duty ratio in BES [10]. The basic function of the buck-boost converter control is to regulate the charging/discharging cycles of the battery and the DC bus voltage.

B. Communication Network for the Proposed Control

A directed graph $\mathcal G$ is used to model the communication network where the nodes represent the agents for the DGs and the edges represent the communication links between nodes [7]. $\mathcal G$ can be represented by a time-invariant adjacency matrix $\mathbf A = [a_{ij}] \in \mathbb R^{N \times N}$. The Laplacian matrix is defined as $\mathbf L = \mathbf D^{\mathrm{in}} - \mathbf A$ where $\mathbf D^{\mathrm{in}} = \mathrm{diag}\{d^{\mathrm{in}}\}$ is the in-degree matrix with $d^{\mathrm{in}} = \sum_{j \in \mathcal N_i} a_{ij}$ and $\mathcal N_i$ as the set of neighbors of node i [7].

Define another matrix $\mathbf{A}' = [a'_{ij}] \in \mathbb{R}^{N \times N}$ with $a'_{ij} = k_j a_{ij}$. Removing the rows and columns in \mathbf{A}' corresponding to the DGs without BES, we get another adjacency matrix $\tilde{\mathbf{A}} = [\tilde{a}_{ij}] \in \mathbb{R}^{\tilde{N} \times \tilde{N}}$ which represents a communication network $\tilde{\mathcal{G}}$ only for the DGs with BES, whose corresponding Laplacian matrix is $\tilde{\mathbf{L}}$. Note that $\tilde{\mathcal{G}}$ is a sub-network of \mathcal{G} and is used for SOC balancing among the DGs with BES.

In this work, it is assumed that each of \mathcal{G} and $\tilde{\mathcal{G}}$ has at least one spanning tree and minimum redundancy, and the Laplacian matrices \mathbf{L} and $\tilde{\mathbf{L}}$ are balanced. Through the communication networks the agents exchange information about active power, DG configuration, and average SOC with neighboring DGs.

III. PROPOSED DISTRIBUTED FREQUENCY CONTROL

The design objectives of the proposed distributed frequency control include: 1) Regulating DG output frequencies to nominal frequency, 2) Achieving SOC balancing among BES units, and 3) Achieving power sharing among hybrid PV-BES plants.

In this study, a droop-free distributed frequency control utilizing a SOC balancing regulator and an adaptive active power sharing regulator is considered. Fig. 2 shows the schematic of the proposed control. The SOC and active power regulators generate frequency correction terms $\Delta\omega_i^2$ and $\Delta\omega_i^2$,

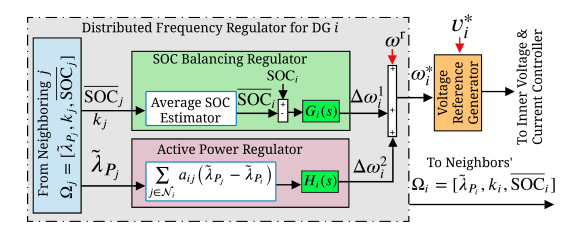


Fig. 2. Proposed distributed frequency control.

respectively, which are then added to the microgrid rated frequency ω^{r} to generate the reference frequency ω_{i}^{*} as:

$$\omega_i^* = \omega^{\rm r} + \Delta \omega_i^1 + \Delta \omega_i^2. \tag{1}$$

For voltage regulation we apply the droop-free distributed control in [7] that generates the voltage magnitude reference v_i^* . Then v_i^* and ω_i^* are used for the voltage reference generation in the lower level controller as [6]:

$$v_{o,i}^*(t) = v_i^*(t)\sin\left(\omega^{\mathrm{r}}t + \theta_i^{1*}(t) + \theta_i^{2*}(t)\right),$$
 (2)

where $\theta_i^{1*}(t) = \int_0^t \Delta \omega_i^1(\tau) \,\mathrm{d} \tau$ and $\theta_i^{2*}(t) = \int_0^t \Delta \omega_i^2(\tau) \,\mathrm{d} \tau$ are the phase angle references.

We use proportional resonant voltage and current control loops for the lower level controller [11], which generate modulating signals so that the PCC voltage and frequency at the output of the inverters follow the voltage reference generated by the proposed distributed secondary control.

A. SOC Balancing Regulator

The SOC of the *i*th BES with $k_i = 1$ is computed as [2]:

$$SOC_{i} = SOC_{i}^{0} - \frac{1}{C_{i}^{BES}} \int i_{ini}^{BES} dt,$$
 (3)

where SOC_i^0 , C_i^BES , and $i_\mathrm{in}^\mathrm{BES}$ are, respectively, the initial SOC, capacity, and output current of the ith battery. Assume the power loss in the DC-DC converter of BES is negligible. Then the output power of the ith BES is $P_i^\mathrm{BES} = P_\mathrm{in}^\mathrm{BES} = V_\mathrm{in}^\mathrm{BES} i_\mathrm{in}^\mathrm{BES}$, where $V_\mathrm{in}^\mathrm{BES}$ is the DC bus voltage at the input side of the converter. Define $\mu_i^\mathrm{BES} = 1/(C_i^\mathrm{BES}V_\mathrm{in}^\mathrm{BES})$, then (3) can be rewritten as:

$$SOC_i = SOC_i^0 - \mu_i^{BES} \int P_i^{BES} dt.$$
 (4)

From (4) it can be seen that SOC can be controlled by regulating the BES power. Since a BES has the limited capacity and deep charging/discharging cycles can lead to battery degradation. In order to prevent over-stressing of a battery and reduce battery degradation, SOC balancing among the BESs needs to be achieved.

In order to achieve SOC balancing, the SOC balancing regulator of the *i*th DG first computes the SOC mismatch as:

$$m_{\text{SOC}_i} = \text{SOC}_i - \overline{\text{SOC}}_i,$$
 (5)

and sends it to an integrator G_i to generate the frequency correction term $\Delta \omega_i^1$.

The \overline{SOC}_i in (5) is the average SOC distributedly estimated at DG i utilizing the actual local SOC and the estimated average SOC of the local and adjacent DGs.

• If $k_i = 0$ for DG i, we set:

$$m_{SOC_i} = SOC_i = \overline{SOC}_i = 0.$$
 (6)

• If $k_i = 1$ for DG i, the average SOC is estimated as:

$$\overline{SOC}_{i}(t) = SOC_{i}(t) + \int_{0}^{t} \sum_{j \in \mathcal{N}_{i}} a'_{ij} (\overline{SOC}_{j} - \overline{SOC}_{i}) d\tau.$$
 (7)

Note that the average SOC estimation in (7) is performed only for the DGs with BES. It has been shown in [7] that \overline{SOC}_i can converge to the true average SOC of the DGs with BES if the communication network $\tilde{\mathcal{G}}$ has a spanning tree and a balanced Laplacian matrix.

B. Active Power Sharing Regulator

The DGs in the microgrid have relatively small ratings. Thus in case of a load change or other disturbances the DGs may be over-stressed, which can be prevented by adopting power sharing in proportion to the DG ratings [6].

Let the active power output of DG i be P_i . For a hybrid PV-BES based DG, the rated power depends on the charging/discharging status of the BES, and can be written as

$$P_i^{\rm r} = P_i^{\rm r,PV} + k_i \operatorname{sgn}(P_i^{\rm BES}) P_i^{\rm r,BES}, \tag{8}$$

where $P_i^{\mathrm{r,PV}}$ and $P_i^{\mathrm{r,BES}}$ are, respectively, the PV and BES rated powers, P_i^{BES} is the BES power, and $\mathrm{sgn}(\cdot)$ is the sign function defined as:

$$\operatorname{sgn}(x) = \begin{cases} -1, & \text{if } x < 0 \\ 0, & \text{if } x = 0 \\ 1, & \text{if } x > 0. \end{cases}$$
 (9)

During charging of the BES of hybrid PV-BES plant i, the battery power P_i^{BES} is negative while during discharging P_i^{BES} is positive. Thus $\mathrm{sgn}(P_i^{\mathrm{BES}})$ is needed to help decide the rated power of the hybrid PV-BES plant according to the charging/discharging status of the BES. Let $\lambda_{P_i} = P_i/P_i^{\mathrm{r}}$ be the normalized active power of the hybrid PV-BES plant i. Then for proportional power sharing, for $\forall i, \forall j=1,\ldots,N$ with $j\neq i$, the DGs need to achieve: $\lambda_{P_i}=\lambda_{P_j}$.

When designing the active power sharing regulator, instead of directly using λ_{P_i} , we actually use $\tilde{\lambda}_{P_i} = P_i/\tilde{P}_i^{\rm r}$ where

$$\tilde{P}_i^{\rm r} = P_i^{\rm r} + P_i^{\rm r,BES} m_{{\rm SOC}_i}.$$
 (10)

The additional term $P_i^{\mathrm{r,BES}} m_{\mathrm{SOC}_i}$ helps achieve faster convergence by adjusting power references according to m_{SOC_i} . For example, when SOC_i is smaller than $\overline{\mathrm{SOC}}_i$ ($m_{\mathrm{SOC}_i} < 0$) the rated power is reduced. Thus the DG can utilize more PV power for charging the batteries by injecting less power to the grid. When $\mathrm{SOC}_i > \overline{\mathrm{SOC}}_i$ ($m_{\mathrm{SOC}_i} > 0$), the rated power is increased so that the DG will inject more power to the grid.

The active power regulator at the ith DG computes the active power sharing mismatch as follows:

$$m_{P_i} = \sum_{j \in \mathcal{N}_i} b \, a_{ij} \big(\tilde{\lambda}_{P_j} - \tilde{\lambda}_{P_i} \big), \tag{11}$$

where the coupling gain b is a design parameter. The active power mismatch term m_{P_i} is then sent to an integrator H_i to generate the frequency correction term $\Delta \omega_i^2$.

IV. STEADY-STATE PERFORMANCE ANALYSIS

In this section, we show that in steady state the hybrid PV-BES based DGs can achieve frequency regulation, SOC balancing among the BESs, and power sharing among all DGs. When the communication network $\tilde{\mathcal{G}}$ has a spanning tree and a balanced Laplacian matrix $\tilde{\mathbf{L}}$, in steady state the average SOC estimator in (7) for i with $k_i=1$ will converge to the true average SOC of the \tilde{N} BES units in the hybrid PV-BES microgrid [7]. Therefore, we have $\overline{\mathbf{SOC}}^{\mathrm{ss}} = \mathbf{KMSOC}^{\mathrm{ss}}$ where $\mathbf{M} \in \mathbb{R}^{N \times N}$ is an averaging matrix with all elements as $1/\tilde{N}$ and $\mathbf{K} = \mathrm{diag}\{k_i\} \in \mathbb{R}^{N \times N}$. Then based on the proposed frequency control in Fig. 2 we have

$$\Delta \omega^{1} = \Delta \omega_{0}^{1} + (t - t_{0})\mathbf{G}(\mathbf{SOC}^{ss} - \mathbf{KMSOC}^{ss}) \quad (12)$$

$$\Delta \omega^2 = \Delta \omega_0^2 - (t - t_0) b \mathbf{H} \mathbf{L} \tilde{\mathbf{P}}^{r^{-1}} \mathbf{p}^{ss}, \tag{13}$$

where $\Delta\omega_0^1$ and $\Delta\omega_0^2$ are the column vectors that carry the integrator outputs at $t=t_0$, which are both $\mathbf{0}_N\in\mathbb{R}^N$ (a vector with all zeros) since before any disturbance it is assumed that the system operates at nominal frequency. $\tilde{\mathbf{P}}^{\mathrm{r}}=\mathrm{diag}\{\tilde{P}_i^r\}\in\mathbb{R}^{N\times N}$ is the power rating matrix of the hybrid PV-BES based DGs and $\mathbf{p}^{\mathrm{ss}}\in\mathbb{R}^N$ is a vector of the steady-state P_i . \mathbf{G} and \mathbf{H} are the diagonal matrices carrying the integrator gains of the SOC balancing regulators $(G_i$'s) and active power sharing regulators $(H_i$'s). Then based on (1) we have

$$\boldsymbol{\omega}^{*ss} = \boldsymbol{\omega}^{r} + (t - t_{0}) \left(\mathbf{G} \left(\mathbf{SOC}^{ss} - \mathbf{KMSOC}^{ss} \right) - b\mathbf{HL}\tilde{\mathbf{P}}^{r^{-1}} \mathbf{p}^{ss} \right). \tag{14}$$

Since (14) holds for all $t \geq t_0$ and provides a constant frequency set-point vector $\boldsymbol{\omega}^{*ss}$, the time-varying part of (14) is zero and thus the frequency is regulated back to nominal frequency. Let $\mathbf{U} = b\mathbf{G}^{-1}\mathbf{H}$, we have

$$(\mathbf{I}_N - \mathbf{K}\mathbf{M})\mathbf{SOC}^{\mathrm{ss}} = \mathbf{UL}\tilde{\mathbf{P}}^{\mathrm{r}^{-1}}\mathbf{p}^{\mathrm{ss}},$$
 (15)

where $\mathbf{I}_N \in \mathbb{R}^{N \times N}$ is an identity matrix. Since $\mathbf{M}(\mathbf{I}_N - \mathbf{K}\mathbf{M}) = \mathbf{0}_{N \times N}$ where $\mathbf{0}_{N \times N} \in \mathbb{R}^{N \times N}$ is a matrix with all zero elements, premultiplying the left-hand side of (15) by $\mathbf{M}^{-1}\mathbf{M}$, we have

$$\mathbf{UL\tilde{P}}^{\mathbf{r}^{-1}}\mathbf{p}^{\mathrm{ss}} = \mathbf{0}_{N}.\tag{16}$$

Substituting (16) into (15), we have $(I_N - KM)SOC^{ss} = 0_N$ and thus for DG i with $k_i = 1$ there is $SOC_i^{ss} = \sum_{i \in \mathcal{N}^{BES}} SOC_i^{ss} / \tilde{N}$, indicating that the proposed control can achieve SOC balancing among the BES units in steady state.

Consequently in steady state the $\tilde{P}_i^{\rm r}$ in (10) reduces to the $P_i^{\rm r}$ in (8), and (16) thus becomes:

$$\mathbf{ULP}^{\mathbf{r}^{-1}}\mathbf{p}^{\mathrm{ss}} = \mathbf{0}_N,\tag{17}$$

where $\mathbf{P^r} = \mathrm{diag}\{P_i^{\mathbf{r}}\} \in \mathbb{R}^{N \times N}$. Premultiplying both sides of (17) by \mathbf{U}^{-1} we have

$$\mathbf{L}\mathbf{P}^{\mathbf{r}^{-1}}\mathbf{p}^{\mathrm{ss}} = \mathbf{0}_{N},\tag{18}$$

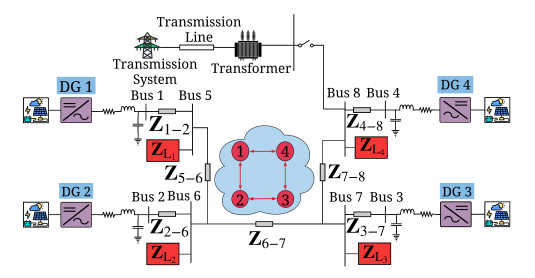


Fig. 3. Schematic diagram of a 4-DG microgrid test system.

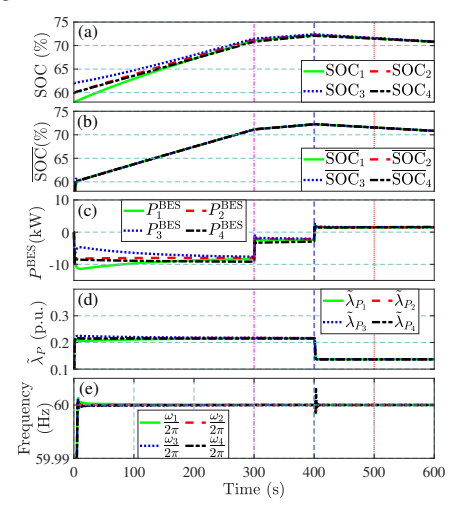


Fig. 4. Control performance of islanded microgrid. (a) SOC of the batteries; (b) Estimated average SOC; (c) Battery output power; (d) Inverter active power sharing; and (e) Frequencies at PCC.

which leads to $\mathbf{p}^{\mathrm{ss}} = m\mathbf{P}^{\mathrm{r}^{-1}}\mathbf{1}_N$ where m is any real number and $\mathbf{1}_N \in \mathbb{R}^N$ is a vector with all ones [7], hinting that the active power sharing is reached in steady state. i.e., $\lambda_{P_i} = \lambda_{P_j}$.

V. OPAL-RT REAL-TIME SIMULATION RESULTS

The performance of the proposed distributed control is validated through real-time simulations in OPAL-RT on a test system system shown in Fig. 3. The power rating of the PVs is $30\,\mathrm{kW}$ and the battery ratings of DG1–DG3 are $15\,\mathrm{Ah}$ and that for DG4 is $17.5\,\mathrm{Ah}$. In this work, all the loads (Z_{L1} – Z_{L4}) are modeled as impedance load. The control performance under islanded and grid-connected modes is considered. In the grid-connected mode a long transmission line connects the microgrid to the AC transmission system. This reduces the AC system inertia and helps the proposed control achieve the frequency regulation objectives. Note that the real-time simulations are performed using OPAL-RT OP4510 at $50\mu s$ sampling.

A. Performance Under Changing Solar Irradiance and Loading Conditions

Fig. 4 shows the controller performance under changing solar irradiance (at 300s and 400s) and loading conditions (at 500s) when the microgrid is disconnected from the grid. It can be seen from Fig. 4 that, although the initial SOCs are different, they converge to the same SOC level at around 300s and despite the irradiance and load change events, the SOCs

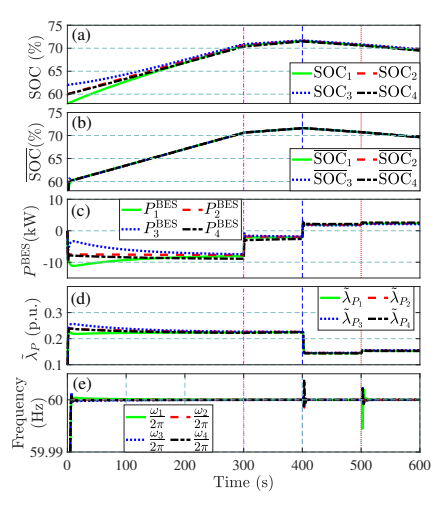


Fig. 5. Control performance of grid-connected microgrid. (a) SOC of the batteries; (b) Estimated average SOC; (c) Battery output power; (d) Inverter active power sharing; and (e) Frequencies at PCC.

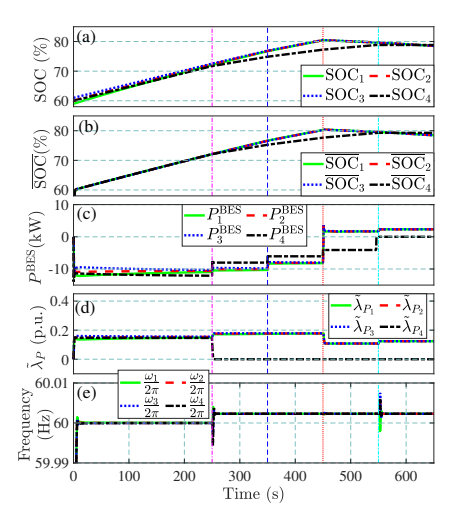


Fig. 6. Control performance of islanded microgrid when DG4 is disconnected at 250 s. (a) SOC of the batteries; (b) Estimated average SOC; (c) Battery output power; (d) Inverter active power sharing; and (e) Frequencies at PCC.

achieve consensus. Also, the proposed control can achieve adaptive frequency regulation and active power sharing under different operating conditions.

We also evaluate the controller performance in the grid-connected mode with identical operating conditions as explained above. In Fig. 5 we apply solar irradiance change at 300s and 400s and AC side load change at 500s. It can be seen that the proposed control successfully achieves the objectives in the grid-connected mode as well.

B. Plug and Play Capability of the Proposed Control

Plug and play capability of the microgrid is essential as the microgrid needs to accommodate disconnection/connection of new sources without interrupting its proper operation with available information from the remaining DGs. For this case study, DG4 in Fig. 3 is intentionally disconnected at 250s. When a DG is disconnected, the communication from that DG becomes unavailable. It is seen from Fig. 6 that the remaining

DG controllers can still successfully achieve their control goals despite the removal of a source under the changes in solar irradiance (at 350s and 450s) and loading conditions (at 550s).

For the impact of communication delay and/or communication loss on the distributed control performance, the readers are referred to [6]. Due to space limit this is not provided here.

VI. CONCLUSION

In this paper, a droop-free distributed frequency control is proposed for the hybrid PV-BES based microgrid. A SOC balancing regulator based on a distributed average SOC estimator is used to achieve a balanced SOC among the DGs with BESs. An active power sharing regulator is used to ensure the proportional active power sharing among all DGs. The performance of the proposed control is validated through real-time simulations in OPAL-RT under disturbances, i.e., changes of solar irradiance and loading conditions. The simulation results demonstrate the controller's performance in successfully achieving frequency regulation, SOC balancing, and active power sharing under varying operating conditions. Our future work will incorporate fault-ride through capabilities, resiliency against cyber-attacks, and unbalance compensation schemes.

REFERENCES

- [1] B. Wang, Y. Wang, Y. Xu, X. Zhang, H. B. Gooi, A. Ukil, and X. Tan, "Consensus-based control of hybrid energy storage system with a cascaded multiport converter in DC microgrids," *IEEE Trans. Sustain. Energy*, vol. 11, no. 4, pp. 2356–2366, Oct. 2020.
- [2] C. Li, E. A. A. Coelho, T. Dragicevic, J. M. Guerrero, and J. C. Vasquez, "Multiagent-based distributed state of charge balancing control for distributed energy storage units in AC microgrids," *IEEE Trans. Ind. Appl.*, vol. 53, no. 3, pp. 2369–2381, May-June 2017.
- [3] S. Augustine, M. K. Mishra, and N. Lakshminarasamma, "A unified control scheme for a standalone solar-PV low voltage DC microgrid system with HESS," *IEEE Trans. Emerg. Sel. Topics Power Electron*, vol. 8, no. 2, pp. 1351–1360, 2020.
- [4] T. Dragičević, J. M. Guerrero, J. C. Vasquez, and D. Škrlec, "Supervisory control of an adaptive-droop regulated DC microgrid with battery management capability," *IEEE Trans. Power Electron.*, vol. 29, no. 2, pp. 695–706, 2014.
- [5] Y. Karimi, H. Oraee, M. S. Golsorkhi, and J. M. Guerrero, "Decentralized method for load sharing and power management in a PV/battery hybrid source islanded microgrid," *IEEE Trans. Power Electron.*, vol. 32, no. 5, pp. 3525–3535, May 2017.
- [6] S. M. Mohiuddin and J. Qi, "Droop-free distributed control for AC microgrids with precisely regulated voltage variance and admissible voltage profile guarantees," *IEEE Trans. Smart Grid*, vol. 11, no. 3, pp. 1956–1967, May 2020.
- [7] V. Nasirian, Q. Shafiee, J. M. Guerrero, F. L. Lewis, and A. Davoudi, "Droop-free distributed control for AC microgrids," *IEEE Trans. Power Electron.*, vol. 31, no. 2, pp. 1600–1617, Feb. 2016.
- [8] M. S. Golsorkhi, Q. Shafiee, D. D.-C. Lu, and J. M. Guerrero, "A distributed control framework for integrated photovoltaic-battery-based islanded microgrids," *IEEE Trans. Smart Grid*, vol. 8, no. 6, pp. 2837– 2848, Nov. 2017.
- [9] H. Cai, J. Xiang, and W. Wei, "Decentralized coordination control of multiple photovoltaic sources for DC bus voltage regulating and power sharing," *IEEE Trans. Ind. Electron.*, vol. 65, no. 7, pp. 5601–5610, Jul. 2018.
- [10] S. Sahoo and S. Mishra, "A multi-objective adaptive control framework in autonomousDC microgrid," *IEEE Trans. Smart Grid*, vol. 9, no. 5, pp. 4918–4929, Sept. 2018.
- [11] C. A. Macana and H. R. Pota, "Adaptive synchronous reference frame virtual impedance controller for accurate power sharing in islanded acmicrogrids: A faster alternative to the conventional droop control," in 2017 IEEE ECCE, Oct. 2017, pp. 3728–3735.